Generation of a nicking enzyme that stimulates site-specific gene conversion from the I-AniI LAGLIDADG homing endonuclease

Audrey McConnell Smith[a,b,c], Ryo Takeuchi[a,c], Stefan Pellenz[c,d], Luther Davis[c,e], Nancy Maizels[b,c,e], Raymond J. Monnat, Jr.[b,c,d], and Barry L. Stoddard[a,b,c,1]

[a]Division of Basic Sciences, Fred Hutchinson Cancer Research Center, 1100 Fairview Avenue, North Seattle, WA 98109; [b]Graduate Program in Molecular and Cellular Biology, University of Washington, Seattle, WA 98195; [c]Northwest Genome Engineering Consortium, Seattle, WA 98101; and Departments of [d]Pathology and Genome Sciences, and [e]Immunology and Biochemisty, University of Washington Medical School, Seattle, WA 98195

Edited by David Baker, University of Washington, Seattle, WA, and approved February 6, 2009 (received for review October 20, 2008)

Homing endonucleases stimulate gene conversion by generating site-specific DNA double-strand breaks that are repaired by homologous recombination. These enzymes are potentially valuable tools for targeted gene correction and genome engineering. We have engineered a variant of the I-AniI homing endonuclease that nicks its cognate target site. This variant contains a mutation of a basic residue essential for proton transfer and solvent activation in one active site. The cleavage mechanism, DNA-binding affinity, and substrate specificity profile of the nickase are similar to the wild-type enzyme. I-AniI nickase stimulates targeted gene correction in human cells, *in cis* and *in trans*, at ≈1/4 the efficiency of the wild-type enzyme. The development of sequence-specific nicking enzymes like the I-AniI nickase will facilitate comparative analyses of DNA repair and mutagenesis induced by single- or double-strand breaks.

protein engineering | recombination | single strand breaks | gene therapy | gene repair

Homing endonucleases generate sequence-specific DNA double-strand breaks (DSBs) that are eventually invaded by their own open reading frames, usually in concert with surrounding intron or intein sequences (1, 2; reviewed in ref. 3). Repair of the break by homologous recombination results in genetic transmission and persistence of these mobile elements (4). Homing endonucleases are promising reagents for catalyzing targeted gene correction or modification because they recognize long DNA target sites (spanning 14–40 bp) with great sequence specificity (5–7; reviewed in refs. 8 and 9). Members of one particular family, the LAGLIDADG homing endonucleases (LHEs), are especially promising because they exhibit the greatest sequence specificity, cleaving as few as 1 in 10^8–10^9 random DNA sequences (10, 11).

LHEs contain two similar core folds of mixed α/β topology. The conserved LAGLIDADG amino acid sequence motifs form two α-helices that are packed together at the domain or subunit interface, where each contributes a catalytic residue to an active site (12). Enzymes containing a single LAGLIDADG motif per protein chain form homodimers that recognize palindromic and pseudopalindromic DNA target sites, whereas proteins containing two motifs form asymmetric monomers that recognize correspondingly asymmetric DNA target sites.

To use LHEs as therapeutic gene correction reagents, it is essential that endonuclease-induced breaks be conservatively repaired. Naturally occurring LHEs create double-strand breaks that can be repaired by either homologous recombination (HR), which uses a homologous donor sequence as a template to repair the damage, or by nonhomologous end joining (NHEJ), which directly rejoins the two free DNA ends (13–16). Homologous recombination occurs without loss of sequence information, whereas NHEJ usually results in sequence loss at the repair junction (15, 17) and can also promote chromosome translocations at DSBs, leading to genomic instability. Several homing endonucleases have been shown to cause such genomic instability as a result of NHEJ-mediated break repair (5, 18–21).

An enzyme that creates nicks rather than DSBs might stimulate homologous recombination while reducing genomic instability associated with DSBs. Although DSBs have an important role as initiators of homologous recombination (22), several models for recombination readily accommodate initiation by nicks (23–26). Some members of the HNH family of homing endonucleases (such as the phage-derived enzyme I-HmuI) cut a single strand of the DNA substrate and promote efficient intron homing (27). Studies in yeast have demonstrated that site-specific nicks can stimulate mitotic interchromosomal recombination (26). Moreover, the ability of nicks to stimulate homologous recombination in mammalian cells has been established by analysis of derivatives of the RAG proteins, which cleave DNA to promote V(D)J recombination at the Ig genes (17).

Naturally occurring restriction enzymes have been engineered to nick DNA at their short recognition sequences by inactivating or replacing one of the two subunits (28–31). An analogous strategy can be applied to convert a monomeric homing endonuclease to a nickase by inactivating one of the two endonuclease active sites. LAGLIDADG endonucleases appear to employ a canonical 2-metal ion mechanism of phosphoryl hydrolysis (Fig. 1*A*) (32, 33). A conserved acidic residue from the C terminus of each catalytic motif coordinates bound metal ions in each of the two active sites, and additional peripheral side chains participate in proton transfer and transition state stabilization. Mutation of these latter residues abrogates DNA cleavage by the homodimeric endonuclease I-CreI (32) and was shown more recently to generate nicking variants of the monomeric endonuclease I-SceI (34). In that study, mutation of either of two active-site lysine residues produced a DNA-nicking enzyme with significant sequence and strand specificity.

Here, we describe engineering a sequence-specific nickase from the monomeric endonuclease I-AniI by mutation of a single residue in the active site, and we demonstrate that the nickase can promote targeted gene correction by homologous recombination in human cells. A comparison of the I-AniI nickase and the parental "cleavase" demonstrates that the two enzymes display similar solution behaviors, metal dependence and pH dependence, DNA target site affinity, and DNA sequence

Author contributions: A.M.S., R.T., S.P., L.D., N.M., R.J.M., and B.L.S. designed research; A.M.S., R.T., S.P., L.D., and B.L.S. performed research; A.M.S., R.T., S.P., and L.D. contributed new reagents/analytic tools; A.M.S., R.T., S.P., L.D., N.M., R.J.M., and B.L.S. analyzed data; and A.M.S., S.P., L.D., N.M., R.J.M., and B.L.S. wrote the paper.

The authors declare no conflict of interest.

This article is a PNAS Direct Submission.

[1]To whom correspondence should be addressed. E-mail: bstoddar@fhcrc.org.

This article contains supporting information online at www.pnas.org/cgi/content/full/0810588106/DCSupplemental.

BIOCHEMISTRY

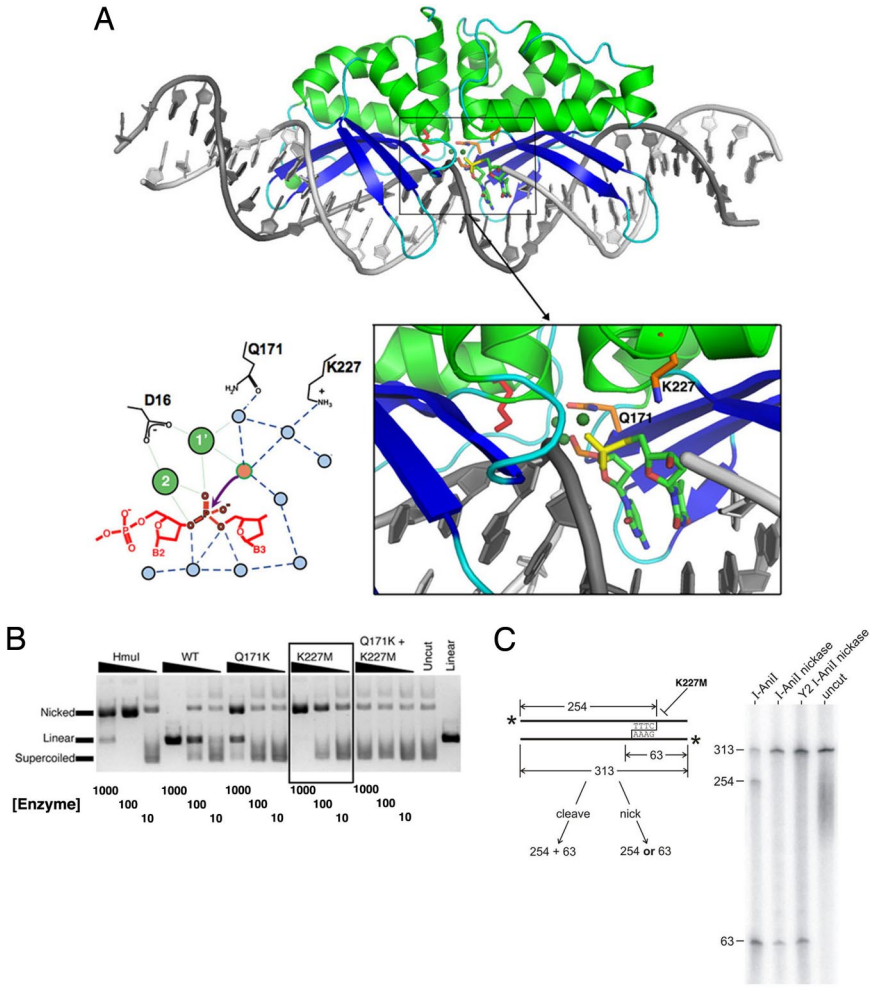

Fig. 1. Point mutations generate an I-AniI nickase. (*A*) (*Upper*) Ribbon diagram of wild-type I-AniI (α-helices, green; β-sheets, blue) bound to its DNA target site (gray). (*Lower*) Attack on the DNA backbone mediated by residues Q171 and K227, in the periphery of the right active site. (*B*) Cleavage of a plasmid substrate containing the Lib4 I-AniI target sequence by wild-type, Q171K, K227M, and Q171K/K227M I-AniI variants at 10, 100, and1000 nM enzyme. Digestion with I-HmuI provides a nicked substrate control; uncut plasmid and EcoRI-linearized plasmid are at the right. The box indicates the strongest nickase, K227M I-AniI. (*C*) Gel electrophoresis of products of cleavage of a 5′ end-labeled 313-bp duplex substrate (*Left*, asterisk, ^{32}P-label) by wild-type I-AniI, I-AniI K227M, and Y2 I-AniI K227M. Predicted radiolabeled fragments of 254 and 63 nucleotides are indicated.

specificity. We also show that the I-AniI nickase stimulates gene conversion in human cells, both *in cis* and *in trans*, and that the nickase active-site mutation can be combined with additional amino acid substitutions in the endonuclease scaffold that increase physiological activity. Nickases similarly engineered from other LHEs may be valuable for a variety of genome engineering applications and as useful reagents for comparing homologous recombination, gene conversion, and mutagenesis stimulated by single- versus double-strand breaks.

Results

Point Mutations to Generate an I-AniI Nickase. I-AniI, encoded by a group I intron harbored within the *Aspergillus nidulans* apocytochrome B oxidase gene, cleaves a 19-bp asymmetric DNA target [supporting information (SI) Fig. S1]. To generate an I-AniI variant with strand-specific nicking activity, we inactivated one of the two catalytic centers responsible for DNA strand cleavage. We focused on three residues at the periphery of the active sites: K94 in the N-terminal domain and Q171 or K227 in the C-terminal domain (Fig. 1*A*). Activity of endonucleases harboring point mutations at these positions was characterized by assaying nicking and relaxation of supercoiled plasmid (Fig. 1*B*) or cleavage of a synthetic DNA duplex substrate (Fig. 1*C*). Both substrates contained an optimized DNA target sequence for in vitro I-AniI cleavage (termed Lib4), which carries substitutions at 2 bp that increase the in vitro binding affinity and cleavage efficiency of native I-AniI (11) (Fig. S1).

The K94M substitution, within the N-terminal active site, did not substantially alter double-strand cleavage activity. The Q171K substitution, within the C-terminal active site, conferred nicking activity (60% of the plasmid substrate was nicked in 2 h with 1 μM enzyme), but also displayed significant double-strand cleavage in extended digests. The K227M substitution, also in the C-terminal active site, exhibited the clearest nicking activity: >99% of the plasmid substrate was nicked in 2 h by 1 μM enzyme, with no detectable linearization after extended incubations. A double mutant harboring both Q171K and K227M substitutions was completely inactive. Based on these results, we used the K227M nickase variant (and the K227M/Q171K "dead" variant as a control) for detailed studies.

To verify the strand specificity of the I-AniI K227M nickase, digests were performed by using a radiolabeled, asymmetric linear DNA duplex containing the I-AniI target site (Fig. 1*C*). I-Ani K227M nickase clearly generated single-strand products of the predicted sizes with little or no cleavage of the complementary DNA strand. The K227M mutation was also incorporated

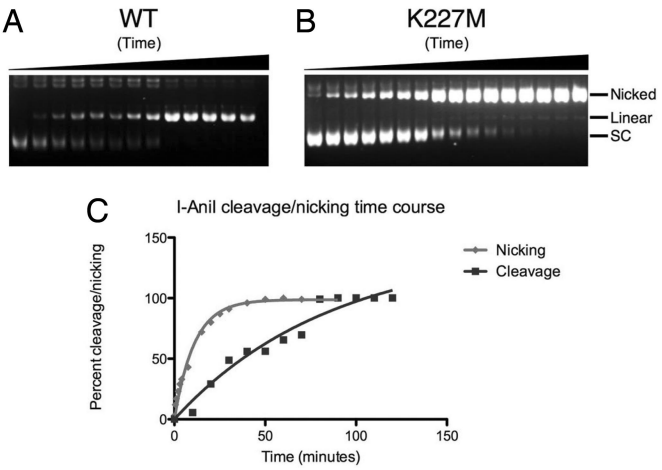

Fig. 2. DNA target site cleavage and nicking by I-AniI and I-AniI nickase. (*A*) Time course of DNA digestion by I-AniI, assayed at 10-min intervals over 2 h. (*B*) Time course of DNA digestion by I-AniI nickase, assayed at 0, 0.5, 1, 2, 3, 4, 7.5, 10, 15, 20, 25, and 30 min, and then at 10-min intervals up to 90 min. (*C*) Plot of reaction time versus percentage cleavage or nicking. Curves fit with program Prism5: nicking $t_{1/2}$ = 7.6 min, cleavage $t_{1/2}$ = 59.6 min.

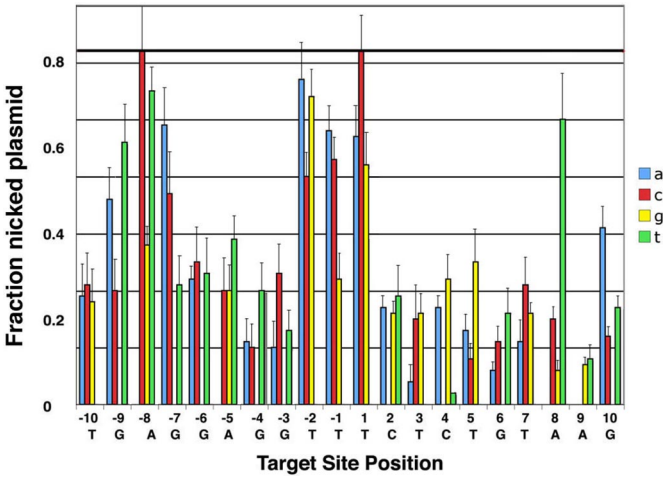

Fig. 3. Specificity profile of I-AniI nickase. Fraction of nicked plasmid substrate recovered is shown for each of 60 targets assayed; indicated colors denote sequence at each position. The bold horizonal line illustrates the relative cleavage of the wild-type target site, measured as a control experiment during each set of digests. Examples of digests are shown in Fig. S4.

into a variant of I-AniI that harbors two additional mutations (F13Y and S111Y, both located far from the active sites; Fig. S1) that increase cleavage activity at physiological temperatures and improve in vivo recombination activity, particularly against the native target site (35). In this Y2 scaffold, the K227M substitution conferred site-specific nicking activity at significantly lower enzyme concentrations (1–10 nM) (Fig. S2). At higher enzyme concentrations, a measurable (although still minor) fraction of the substrate was eventually converted to linearized product.

In Vitro Activity Comparison of Wild-Type I-AniI and the I-AniI K227M Nickase. The activities of native I-AniI cleavase and K227M I-AniI nickase were measured over a pH range of 5.0–10.5. At protein concentrations in excess of the enzymatic K_d, wild-type I-AniI exhibited optimal activity at pH 9.0, and the K227M nickase exhibited maximal activity at slightly lower pH (≈pH 8.0; Fig. S3 *A* and *B*). Both wild-type I-AniI and the I-AniI K227M nickase exhibited optimal activity at 5 mM $MgCl_2$ (Fig. S3 *C* and *D*).

Isothermal titration calorimetry was used to determine the dissociation constants for the I-AniI cleavase, nickase, and a catalytically inactive I-AniI variant on the Lib4 DNA target site (Fig. S3*E*), as described in ref. 36. We obtained average values for the enzyme dissociation constant (K_d) of 8 nM for the wild-type enzyme, 71 nM for I-AniI K227M nickase, and 62 nM for the catalytically inactive variant. The nickase exhibited an increase of +1.4 kcal/mol in $\Delta G_{binding}$ compared with wild-type enzyme. This difference is primarily the result of a +5.8 kcal/mol increase in enthalpy change upon nickase binding, implying that the I-AniI K227M nickase has reduced contact with the DNA target, presumably because a hydrogen bond formed by the K227 side chain to the DNA phosphate backbone (11) is eliminated.

The relative rates of DNA cleavage by wild-type I-AniI and the I-AniI K227M nickase were determined (Fig. 2) at 1 μM enzyme, a concentration ≈100- and 10-fold higher than the respective dissociation constants, and thus reporting on differences in the rate-limiting steps of the reactions. The rate of nicking was ≈8-fold faster than cleavage, exhibiting a $t_{1/2}$ of 7.6 min compared with 59.6 min for cleavage by the wild-type enzyme. The wild-type enzyme is likely limited by a need to undergo conformational changes between sequential top- and bottom-strand cleavage events, including altered metal ion coordination in the active sites during cleavage of the two DNA strands. Recently solved structures of I-SceI reaction intermediates illustrate such catalytic center metal rearrangements occurring between strand cleavage events (33).

A previous analysis of I-AniI DNA cleavage specificity, using recovery of linearized products from a randomized, plasmid-encoded target site library, estimated the overall specificity of I-AniI to be ≈1 in 10^8 under ideal cleavage conditions (11). A similar screen was not possible for the engineered I-AniI K227M nickase because of the low background of nonenzymatically nicked substrates in plasmid preparations. Therefore, we measured the specificity profile by assaying the relative nicking of every possible variant of the I-AniI target site (Fig. 3). This corresponded to 60 mutated sequences, comprising all three possible base pair substitutions at each of 20 positions across the target (Fig. S4). The cleavage specificity profile of I-AniI K227M nickase was quite similar to that observed for the wild-type enzyme. Specificity is greatest across base pair positions ±3, 4, 5, and 6 in each half-site, where the enzyme makes a majority of target site DNA base-specific contacts via the major groove. The enzyme is least specific across 3 of 4 bases at the center of the target, positions −2 to +1, where the enzyme straddles the DNA minor groove and contacts predominantly the DNA backbone. Specificity is also low at the outer flanks of each half-site, where the enzyme makes less saturated contacts to individual bases. The similarity between specificity profiles of wild-type I-AniI and the I-AniI K227M nickase indicates that target site recognition is not significantly affected by the K227M substitution.

Comparison of Recombination in Vivo Stimulated by the I-AniI Cleavage or Nicking Activities. We developed assays to quantify endonuclease-mediated gene correction, by using either intramolecular recombination of a reporter *in cis* or recombination of a chromosomal target with a donor allele *in trans* (Fig. 4 and Tables S1 and S2). The assay for recombination *in cis* used a plasmid-encoded reporter, DR-GFPAni, that contains a direct repeat of two inactive GFP alleles (Fig. 4*A*) (37). The corresponding assay for gene correction *in trans* measures correction of a defective, chromosomally integrated GFP target transgene by an exogenous truncated GFP repair template (Fig. 4*B*). This latter assay quantitates cleavage-dependent repair under conditions that closely resemble potential therapeutic gene targeting or repair reactions and gives a much lower background of GFP^+

BIOCHEMISTRY

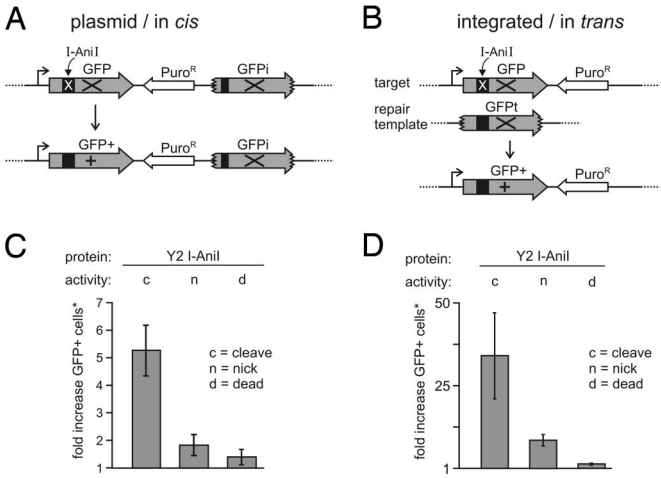

Fig. 4. In vivo recombination stimulated by I-AniI cleavase or nickase. (*A*) Reporter assay for recombination *in cis.* Recombination of an inactive 3′-GFP gene (GFPi) with a cleaved 5′-GFPi allele generates a functional GFP$^+$ gene. Gray arrows, GFP alleles; filled box with white X, I-AniI cleavage site and stop codon; arrow, promoter; Puro^R, selectable puromycin resistance marker. (*B*) Reporter assay for recombination *in trans.* Recombination of a chromosomally integrated target with a transfected repair template (GFPt) generates a functional GFP$^+$ gene. GFP$^+$ alleles and cells in both assays are detected and quantified by flow cytometry. Other notations are as in *A*. (*C*) Fold increase in the frequency of GFP$^+$ cells in the *cis* assay shown in *A* above, relative to reporter-only background, after expression of Y2 I-AniI cleavase (c), Y2 I-AniI nickase (n), or catalytically inactive Y2 I-AniI nickase (d). Additional primary data are presented in Table S1. (*D*) Fold increase in the frequency of GFP$^+$ cells in the *trans* assay shown in *B* above, relative to reporter-only background, after expression of Y2 I-AniI cleavase (c), Y2 I-AniI nickase (n), or a catalytically inactive form of Y2 I-AniI nickase (d). Additional primary data are presented in Table S1.

cells ($\leq 3 \times 10^{-5}$; Tables S1and S2) in the absence of endonuclease expression.

For the assay conducted *in cis* (Fig. S5), human 293T fibroblasts were transiently cotransfected with a DR-GFPAni reporter plasmid containing an I-AniI target site in the 5′-GFP allele and a plasmid expressing either I-AniI harboring double-strand break activity (native cleavase), single-strand break activity (K227M; nickase), or no cleavage activity (K227M/Q171K; dead). GFP$^+$ cells were quantified by fluorescence-activated cell sorting. Transfection efficiency was assessed by transfection with a pEGFP-N1 control plasmid and was consistently high (mean 95%). Levels of expression of the various I-AniI constructs were comparable, as verified by Western blotting (Fig. S6). In these assays (Fig. 4*C* and Table S1), the expression of a catalytically inactive endonuclease construct results in a slight increase (1.3-fold) in formation of GFP$^+$ cells over the reporter-only background. This may reflect the background frequency of DNA replication across the reporter, because previous studies have demonstrated that tightly bound DNA-binding proteins (as well as other types of modifications and lesions) can act as a barrier to the replication fork, leading to double-strand breaks (reviewed in ref. 38). The expression of the nickase in the same system only slightly increases the generation of GFP+ cells (1.8-fold over background) beyond the effect observed for the inactive enzyme. In contrast, the native cleavage activity results in a more significant increase (5.2-fold) in recombination and gene conversion. Both the I-AniI cleavase and nickase were more active on reporter plasmids containing the native as opposed to the Lib4 target site (Table S1), a result that agrees with in vivo activity measurements on the two target sites in previous studies (35).

For the assay conducted *in trans* (Fig. 4*D* and Table S2), human 293T cells carrying the stable integrated target were generated by transfection with the pZF-GFPAni plasmid followed by puromycin selection. Transfection of 293T/ZF-GFPAni cells with either the repair template DNA alone or an I-AniI expression vector alone did not lead to the generation of GFP$^+$ cells above background levels ($\leq 3 \times 10^{-5}$; Table S2). As was observed in experiments using the *cis* reporter system, expression of the Y2 I-AniI catalytically inactive dead mutant slightly stimulated the generation of GFP$^+$ cells, ≈1.3-fold over background levels. In contrast, cotransfection with the repair template and the Y2 I-AniI nickase expression construct stimulated gene correction ≥8-fold; and cotransfection with the repair template and the Y2 I-AniI cleavase stimulated gene correction up to 35-fold (Fig. 4*D* and Table S2). The 4-fold difference between stimulation of recombination *in trans* by the Y2 I-AniI cleavase and nickase parallels the difference observed in the *cis* recombination assays described above, despite substantial differences in absolute recombination frequencies.

Discussion

Previous experiments have demonstrated that Y2 I-AniI is similar in recombination and gene conversion activity in transfected mammalian cells to the I-SceI endonuclease (35), which has a long history of use in such experiments (5, 7, 8). We have converted the I-AniI endonuclease to a nickase, without a significant reduction in enzyme specific activity or sequence specificity of cleavage. The I-AniI K227M nickase is very active, nicking its DNA target site ≈8-fold faster than wild-type I-AniI generates a DSB. Thus, the nickase maintains or improves on the specificity and activity of the I-AniI cleavase to provide a protein with properties desirable for potential therapeutic application.

Conversion of I-AniI to a nickase takes advantage of a natural asymmetry in DNA cleavage that is often displayed by monomeric LHEs. The algal endonuclease I-CpaII displays metal ion-dependent asymmetric cleavage, preferentially nicking the bottom strand of its target site at very low magnesium (39). The yeast homing endonuclease I-SceI has higher affinity for binding to the 3′ DNA half-site, leading to accumulation of nicked intermediates during the cleavage reaction (40). Finally, the archaeal endonuclease I-DmoI preferentially cleaves the coding strand of its host gene (41), a preference that can be enhanced further by mutation of the LAGLIDADG motif (42).

The mutational strategy used to generate the I-AniI nickase was dictated by the catalytic mechanism of this and related LHEs. Mutation of metal-binding residues within the LAGLIDADG motif causes significant disruption of the endonuclease active site and loss of DNA-binding affinity. In contrast, mutation of more distant polar side chains involved in solvent-mediated interactions and proton transfer (Q47 and K98 in I-CreI; Q171 and K227 in the C-terminal domain of I-AniI) causes significant reductions in catalytic efficiency with little effect on either overall affinity or the structure of the enzyme–DNA complex (32). In the related LHE, I-SceI, substitution of pseudosymmetric residues K122 and K223 similarly revealed nickase activity (34). The availability of multiple LHE scaffolds for the creation of site-specific nickases should facilitate future studies of DNA repair and recombination in response to single- vs. double-strand breaks.

I-AniI nickase was able to stimulate homologous recombination in human cells with an efficiency ≈1/4 that of wild-type I-AniI enzyme, measured either in transient recombination assays *in cis* or in chromosomal gene correction assays *in trans.* To minimize the formation of DSBs after nicking (as a result of DNA replication), the DR-GFPAni reporter plasmids used for transient recombination assays do not contain elements known to drive replication in human cells, and the *trans* recombination assays were conducted under conditions that involve minimal cell division. Therefore, it seems possible that

recombination in these assays, in the presence of the nickase, involves minimal formation of replicative DSBs. It should be possible to verify this by establishing whether there are distinct genetic requirements for recombination induced by the I-AniI nickase and cleavase. Recombination initiated by nicks as opposed to DSBs has not been systematically studied, in part because there is a paucity of reagents that reliably nick DNA in vivo in a site-specific fashion. The availability of nickase variants of I-AniI and of I-SceI (34) should facilitate mechanistic analyses of nick or break processing that lead to the generation of recombinant molecules.

A sequence-specific nickase, such as the I-AniI variant described in this work, has particular promise for therapeutic applications, including the targeted repair of human disease-causing mutations. Although DSBs may stimulate homologous recombination more efficiently than nicks, they are also more likely to promote mutagenic repair or potentially deleterious genome rearrangements at the endonuclease-induced break site (5, 18–21). It may be possible to avoid such deleterious events by initiating recombinational repair with a site-specific nick, rather than a DSB. Thus, engineered nickase variants of I-AniI and other homing endonucleases may be particularly useful reagents not only for targeted genome engineering but also therapeutic gene repair.

Methods

Protein Expression, Purification, and Mutagenesis. Expression and purification protocols were similar to those described in ref. 43. All I-AniI scaffolds included the F80K and L233K mutations, shown to improve solution behavior of the enzyme (11). The Y2 variant contains two additional mutations, F13Y and S111Y, which enhance both DNA-binding affinity and cleavage efficiency at physiological temperatures (35). All I-AniI point mutants were generated by QuikChange XL (Stratagene). Oligonucleotides (Operon) used to generate K227M were 5′-CAAAATGCGCCTGTCAAATTATTAGGGAATATGAAATTA-CAATATAAATTATGGTTAAAAC-3′ and its complement; and to generate Q171K were 5′-CGCTAGTTTTGATATTGCTAAACGCGATGGGGATATTCTG-3′ and its complement. All expression constructs were verified by direct sequencing.

Cleavage and Nicking Assays. Cleavage was carried out as described in ref. 11 in reactions containing 10 nM Lib4 I-AniI target site in BlueScript plasmid substrate and 1 μM I-AniI, unless otherwise specified; this enzyme concentration is well over K_d for the interaction between I-AniI and its DNA target site. Most reactions were carried out in 50 mM Tris (pH 7.5), 100 mM NaCl, 10 mM $MgCl_2$, and 1 mM DTT and incubated at 37 °C for 2 h and terminated by the addition of an equal volume of 2× stop buffer [2% SDS (vol/vol), 100 mM EDTA, 20% (vol/vol) glycerol, and 0.2% bromophenol blue]. Control digests with EcoRI and the nickase I-HmuI were performed under the same conditions. For pH profiles, Tris was substituted by sodium citrate (pH 5.0, 5.5), Bistris (pH 6.0, 6.5), Tris (pH 7.0–9.0), and Caps (pH 9.5–10.5). Reactions for pH profiles and magnesium titrations were terminated before complete substrate digestion had occurred.

To generate the 313-bp duplex cleavage substrate, an I-AniI Lib4 target site was amplified from pBS using primers SP149 (5′-CGTAATACGACTCACTAT-AGG-3′) and SP150 (5′-CGCAATTAATGTGAGTTAGCT-3′), products purified on Illustra ProbeQuant G-50 columns (GE Healthcare), and 5′ end-labeled with [γ-^{32}P]ATP (PerkinElmer) and T4 polynucleotide kinase (NEB) according to the manufacturers' protocols. After cleavage in a 10-μL reaction, 2 μL of 5× stop solution [0.1 M Tris·HCl (pH 7.5), 0.25 M EDTA, 5% SDS] was added, and samples were denatured at 95 °C for 5 min with deionized formamide, 0.1% xylene cyanol, and 0.1% bromophenol blue, quick-chilled, and then resolved by electrophoresis on a 6% polyacrylamide denaturing gel. Gels were dried and analyzed by phosphorimaging.

Nicking Site Specificity. A substrate matrix of I-AniI target sites for determination of nickase specificity was created and generously provided by Summer Thyme (University of Washington, Seattle). The substrate matrix was generated by cloning a synthetic double-stranded 40-bp DNA cassette containing the wild-type I-Ani target sequence (11) into the EcoRI and XhoI sites of the pBlueScript plasmid vector, then creating all three possible substitutions at each of 20 positions by QuikChange site-directed mutagenesis, to generate 60 separate target site variants, which were verified by chemical sequencing. Nicking was assayed in reactions containing 5 nM DNA and 20 nM I-AniI K227M nickase, using a single-enzyme preparation to ensure uniformity. For each substrate, nonenzymatic hydrolysis was quantified in a control reaction in the absence of enzyme.

In Vivo Recombination Assays. Reporter plasmids pDR-GFPAni and pDR-GFPLib4 were constructed by modifying the original pDR-GFP recombination reporter (37). The I-SceI recognition site in the 5′-SceGFP cassette was replaced by cloning into the I-SceI site a synthetic duplex containing SacI, KpnI, and XhoI cleavage sites, generated by annealing oligonucleotides Usrf, 5′-GAGCTCGG-TACCCTCGAGGCCGGACACGCTGAACTTG-3′, and Usrr, 5′-CTCGAGGGTAC-CGAGCTCACCTACGGCAAGCTGACC-3′. This plasmid was then cleaved with SacI and XhoI, and the following annealed duplexes were inserted to generate pDR-GFPAni or pDR-GFPLib4, respectively: Anif, 5′-TCGATGAGGAGGTT-TCTCTGTAAAGCT-3′ and Anir, 5′-TTACAGAGAAACCTCCTCA-3′; or Lib4f, 5′-TCGATGAGGAGGTTACTCTGTTATAACAGCTGAGCT-3′ and Lib4r, 5′-CAGCT-GTTATAACAGAGTAACCTCCTCA-3′.

Plasmid pZF-GFPAni was constructed from pDR-GFP by removal of the downstream, truncated GFP gene by partial HindIII digestion and religation, insertion of the MboI fragment containing a ≈4-kb poly-*lacO* array from plasmid φV-lacO-His (44) into the NotI site downstream of the 5′ SceGFP cassette, and insertion of a duplex containing the Lib4 site, generated by annealing oligonucleotides AniCut.F1, 5′-GGTGAGGAGGTTACTCTGTTAT-AGGGATAA-3′ and AniCut.R1, 5′-CCCTATAACAGAGTAACCTCCTCACCT-TAT-3′ into the I-SceI site. The downstream, truncated GFP gene was excised by HindIII digestion from pDR-GFP and cloned into the HindIII site of pBS-SK$^+$ to generate the truncated GFP donor plasmid, iGFP.

The I-AniI coding plasmids, pCSOMpEFHA-2ndGenNLS-HyperAniKWPRE and pRRLSIN.cPPT.hPGK.HA.2ndGenNLS.reoAniY2 were provided by Michael Certo and Andrew Scharenberg (Seattle Children's Hospital, Seattle, WA). In these, a pEF1α promoter drives I-AniI ORFs that include an N-terminal HA tag and NLS, and the ORF contains F80K and L232K substitutions as well as a silent mutation (G25G) that was necessary to abolish a cryptic splice site (Jordan Jarjour and Andrew Scharenberg, personal communication). This ORF was codon-optimized for expression in mammalian cells and therefore different in sequence from the bacterial expression ORF used for in vitro experiments. The I-AniI nickase ORF contains the additional K227M substitution, constructed by QuikChange using oligonucleotide 5′-CCTGTCAAATTGTTAGGCAACAtGAAACTGCAATACAAGTTG-TGG-3′ and its complement. Catalytically inactive I-AniI contains the additional Q171K mutation, also constructed by QuikChange using oligonucleotide 5′-GATAGCTAGCTTTGACATTGCAAAAAGAGATGGGGATATTT-TAATATCAGCG-3′ and its complement. The latter Y2 scaffold also contains the F13Y and S111Y mutations. For transfections, human 293T cells were grown in Dulbecco's modified Eagle's medium (Cellgro) supplemented with 10% FBS (Cellgro) and 1% penicillin/streptomycin (Gibco) at 37 °C, 5% CO_2. In all cases, transfection efficiency was measured by using the pEGFP-N1 control vector (Clontech). Transient transfections (45) were performed in 24-well plates by using cells plated 24 h before transfection at 3×10^5 cells per well in 500 μL of medium, corresponding to 50–80% confluence, and used 1.5 μg of total DNA and a 3:1 molar ratio of expression plasmid to respective reporter target plasmids. Cells were resuspended by trypsin treatment, and 5×10^5 cells were washed with PBS, stained by incubation in 500 μL of PBS containing 10 ng/μL propidium iodide, and analyzed on an influx flow cytometer (Cytopeia). Typically, 40,000 events were scored and gated first for log side and linear forward scatter to identify cells and then for propidium iodide exclusion to identify viable cells for GFP fluorescence analysis. Assays were performed both with and without propidium iodide staining.

In the targeted gene correction assays, transfections were performed by using Lipofectamine LTX (Invitrogen) according to the manufacturer's protocol; 225 ng of each of two plasmids was transfected, either donor and pBS-SK$^+$ or donor and I-AniI expression plasmid; and after 72 h culture, cells were trypsin treated and resuspended in PBS + 2% formaldehyde. Cells were analyzed on a FACScan flow cytometer (Becton Dickinson). Typically, 75,000 events were gated for linear side and forward scatter to identify cells and then analyzed to determine GFP fluorescence.

ACKNOWLEDGMENTS. We thank members of the Northwest Genome Engineering Consortium who provided advice and reagents. This work was supported by National Institutes of Health Grants R01 GM49857 and RL1 CA133833 (to B.L.S.), 1RL1CA133831 (to R.J.M.), and RL1 GM084434 (to N.M.) and the Gates Foundation Grand Challenges Program award (to B.L.S. and R.J.M.). A.M.S. is supported by a National Science Foundation graduate fellowship. R.T. was supported by a fellowship from the Japan Society for the Promotion of Science.

1. Jacquier A, Dujon B (1985) An intron-encoded protein is active in a gene conversion process that spreads an intron into a mitochondrial gene. *Cell* 41:383–394.
2. Colleaux L, et al. (1986) Universal code equivalent of a yeast mitochondrial intron reading frame is expressed into *E. coli* as a specific double strand endonuclease. *Cell* 44:521–533.
3. Stoddard BL (2005) Homing endonuclease structure and function. *Q Rev Biophys* 38:49–95.
4. Plessis A, Perrin A, Haber JE, Dujon B (1992) Site-specific recombination determined by I-SceI, a mitochondrial group I intron-encoded endonuclease expressed in the yeast nucleus. *Genetics* 130:451–460.
5. Rouet P, Smih F, Jasin M (1994) Expression of a site-specific endonuclease stimulates homologous recombination in mammalian cells. *Proc Natl Acad Sci USA* 91:6064–6068.
6. Rouet P, Smih F, Jasin M (1994) Introduction of double-strand breaks into the genome of mouse cells by expression of a rare-cutting endonuclease. *Mol Cell Biol* 14:8096–8106.
7. Choulika A, Perrin A, Dujon B, Nicolas JF (1995) Induction of homologous recombination in mammalian chromosomes by using the I-SceI system of *Saccharomyces cerevisiae*. *Mol Cell Biol* 15:1968–1973.
8. Paques F, Duchateau P (2007) Meganucleases and DNA double-strand break-induced recombination: Perspectives for gene therapy. *Curr Gene Ther* 7:49–66.
9. Stoddard BL, Monnat RJ, Scharenberg, AM (2007) Advances in engineering homing endonucleases for gene targeting: 10 years after structures. *Progress Gene Ther* 3:135–168.
10. Gimble FS, Moure CM, Posey KL (2003) Assessing the plasticity of DNA target site recognition of the PI-SceI homing endonuclease using a bacterial two-hybrid selection system. *J Mol Biol* 334:993–1008.
11. Scalley-Kim M, McConnell-Smith A, Stoddard BL (2007) Coevolution of a homing endonuclease and its host target sequence. *J Mol Biol* 372:1305–1319.
12. Chevalier B, Monnat RJ, Stoddard BL (2005) in *Homing endonucleases and inteins*, eds Belfort M, Wood D, Derbyshire V, Stoddard B (Springer, Berlin), Vol 16, pp 34–47.
13. Wyman C, Kanaar R (2006) DNA double-strand break repair: All's well that ends well. *Annu Rev Genet* 40:363–383.
14. Sung P, Klein H (2006) Mechanism of homologous recombination: Mediators and helicases take on regulatory functions. *Nat Rev Mol Cell Biol* 7:739–750.
15. Paques F, Haber JE (1999) Multiple pathways of recombination induced by double-strand breaks in *Saccharomyces cerevisiae*. *Microbiol Mol Biol Rev* 63:349–404.
16. Brugmans L, Kanaar R, Essers J (2007) Analysis of DNA double-strand break repair pathways in mice. *Mutat Res* 614:95–108.
17. Lee GS, Neiditch MB, Salus SS, Roth DB (2004) RAG proteins shepherd double-strand breaks to a specific pathway, suppressing error-prone repair, but RAG nicking initiates homologous recombination. *Cell* 117:171–184.
18. Weinstock DM, Richardson CA, Elliott B, Jasin M (2006) Modeling oncogenic translocations: Distinct roles for double-strand break repair pathways in translocation formation in mammalian cells. *DNA Repair* 5:1065–1074.
19. Monnat RJ, Jr, Hackmann AF, Cantrell MA (1999) Generation of highly site-specific DNA double-strand breaks in human cells by the homing endonucleases I-PpoI and I-CreI. *Biochem Biophys Res Commun* 255:88–93.
20. Guirouilh-Barbat J, *et al*. (2004) Impact of the KU80 pathway on NHEJ-induced genome rearrangements in mammalian cells. *Mol Cell* 14:611–623.
21. Allen C, Miller CA, Nickoloff JA (2003) The mutagenic potential of a single DNA double-strand break in a mammalian chromosome is not influenced by transcription. *DNA Repair* 2:1147–1156.
22. Szostak JW, Orr-Weaver TL, Rothstein RJ, Stahl FW (1983) The double-strand break repair model for recombination. *Cell* 33:25–35.
23. Holliday R (1964) A mechanism for gene conversion in fungi. *Genet Res* 5:282–304.
24. Meselson MS, Radding CM (1975) A general model for genetic recombination. *Proc Natl Acad Sci USA* 72:358–361.
25. Radding CM (1982) Homologous pairing and strand exchange in genetic recombination. *Annu Rev Genet* 16:405–437.
26. Strathern JN, Weinstock KG, Higgins DR, McGill CB (1991) A novel recombinator in yeast based on gene II protein from bacteriophage f1. *Genetics* 127:61–73.
27. Landthaler M, Shen BW, Stoddard BL, Shub DA (2006) I-BasI and I-HmuI: Two phage intron-encoded endonucleases with homologous DNA recognition sequences but distinct DNA specificities. *J Mol Biol* 358:1137–1151.
28. Zhu Z, Samuelson JC, Zhou J, Dore A, Xu SY (2004) Engineering strand-specific DNA nicking enzymes from the type IIS restriction endonucleases BsaI, BsmBI, and BsmAI. *J Mol Biol* 337:573–583.
29. Xu SY, et al. (2007) Discovery of natural nicking endonucleases Nb.BsrDI and Nb.BtsI and engineering of top-strand nicking variants from BsrDI and BtsI. *Nucleic Acids Res* 35:4608–4618.
30. Samuelson JC, Zhu Z, Xu SY (2004) The isolation of strand-specific nicking endonucleases from a randomized SapI expression library. *Nucleic Acids Res* 32:3661–3671.
31. Heiter DF, Lunnen KD, Wilson GG (2005) Site-specific DNA-nicking mutants of the heterodimeric restriction endonuclease R. BbvCI. *J Mol Biol* 348:631–640.
32. Chevalier B, et al. (2004) Metal-dependent DNA cleavage mechanism of the I-CreI LAGLIDADG homing endonuclease. *Biochemistry* 43:14015–14026.
33. Moure CM, Gimble FS, Quiocho FA (2008) Crystal structures of I-SceI complexed to nicked DNA substrates: Snapshots of intermediates along the DNA cleavage reaction pathway. *Nucleic Acids Res* 36:3287–3296.
34. Niu Y, Tenney K, Li H, Gimble FS (2008) Engineering variants of the I-SceI homing endonuclease with strand-specific and site-specific DNA-nicking activity. *J Mol Biol* 382:188–202.
35. Takeuchi R, Certo M, Caprara MG, Scharenberg AM, Stoddard BL (December 2008) Optimization of in vivo activity of a bifunctional homing endonuclease and maturase reverses evolutionary degradation. *Nucleic Acids Res*, 10.1093/nar/gkn1007.
36. Eastberg JH, et al. (2007) Thermodynamics of DNA target site recognition by homing endonucleases. *Nucleic Acids Res* 35:7209–7221.
37. Pierce AJ, Johnson RD, Thompson LH, Jasin M (1999) XRCC3 promotes homology-directed repair of DNA damage in mammalian cells. *Genes Dev* 13:2633–2638.
38. McGlynn P, Lloyd RG (2002) Recombinational repair and restart of damaged replication forks. *Nat Rev Mol Cell Biol* 3:859–870.
39. Turmel M, Mercier JP, Cote V, Otis C, Lemieux C (1995) The site-specific DNA endonuclease encoded by a group I intron in the *Chlamydomonas pallidostigmatica* chloroplast small subunit rRNA gene introduces a single-strand break at low concentrations of Mg^{2+}. *Nucleic Acids Res* 23:2519–2525.
40. Perrin A, Buckle M, Dujon B (1993) Asymmetrical recognition and activity of the I-SceI endonuclease on its site and on intron–exon junctions. *EMBO J* 12:2939–2947.
41. Agaard C, Awayez MJ, Garrett RA (1997) Profile of the DNA recognition site of the archaeal homing endonuclease I-DmoI. *Nucleic Acids Res* 25:1523–1530.
42. Silva GH, Belfort M (2004) Analysis of the LAGLIDADG interface of the monomeric homing endonuclease I-DmoI. *Nucleic Acids Res* 32:3156–3168.
43. Bolduc JM, et al. (2003) Structural and biochemical analyses of DNA and RNA binding by a bifunctional homing endonuclease and group I intron splicing factor. *Genes Dev* 17:2875–2888.
44. Cummings WJ, et al. (2007) Chromatin structure regulates gene conversion. *PLoS Biol* 5:e246.
45. Chen C, Okayama H (1987) High-efficiency transformation of mammalian cells by plasmid DNA. *Mol Cell Biol* 7:2745–2752.